7 Histology for Transbronchial Lung Cryobiopsy Samples

Tamiko Takemura, Tomohisa Baba, Takashi Niwa, and Takashi Ogura

7.1 Introduction

Transbronchial lung cryobiopsy (TBLC) is now recognized as a useful tool for the diagnosis of diffuse interstitial lung diseases [1–5], although surgical lung biopsy (SLB) still remains the standard diagnostic procedure [6, 7].

The lung tissue specimens obtained by TBLC are usually smaller than those obtained by SLB [8]. It is important for pathological diagnosis to recognize the anatomical location of structures in the obtained lung tissue specimens. In this chapter, we present a comparison of normal lung tissue samples and representative specimens obtained by cryobiopsy, in the viewpoint of lung architecture.

7.1.1 Processing of Cryobiopsy Specimens

The frozen lung tissue samples are immersed in saline, and the thawed lung specimens are transferred into a 20-mL syringe containing a small amount of saline and inflated by slow application of negative pressure for 30–60 s. After this process, the alveoli are well inflated and eligible for histopathological examination. Figure 7.1 shows well-inflated lung tissue specimens measuring up to about 7 mm in diameter, as compared with the specimens containing non-inflated alveoli.

As for the staining, we recommend elastic van Gieson (EVG) staining and Alcian blue staining in addition to hematoxylin-eosin staining. EVG staining is necessary to recognize the normal and remodeled pulmonary architecture. Alcian blue staining is also useful to detect immature fibrosis such as fibroblastic foci containing much glycoprotein.

7.1.2 Normal Structure of the Lobules and Acini in TBLC Specimens

What are the structures that can be obtained by TBLC? Figure 7.2 shows a Softex image of the peripheral lung tissue, indicating the area from which TBLC specimens are obtained. Usually the cryoprobe is inserted into a membranous bronchiole through the bronchus and pulled 1 cm from the chest wall. The area sampled by the cryoprobe includes the membranous and respiratory bronchioles and peribronchiolar alveoli and

T. Takemura (✉)
Department of Pathology, Japanese Red Cross Medical Center, Tokyo, Japan
e-mail: byori@med.jrc.or.jp

T. Baba · T. Niwa · T. Ogura
Department of Respiratory Medicine, Kanagawa Cardiovascular and Respiratory Center, Yokohama, Japan
e-mail: baba@kanagawa-junko.jp; niwa@kanagawa-junko.jp; ogura@kanagawa-junko.jp

V. Poletti (ed.), *Transbronchial cryobiopsy in diffuse parenchymal lung disease*,
https://doi.org/10.1007/978-3-030-14891-1_7

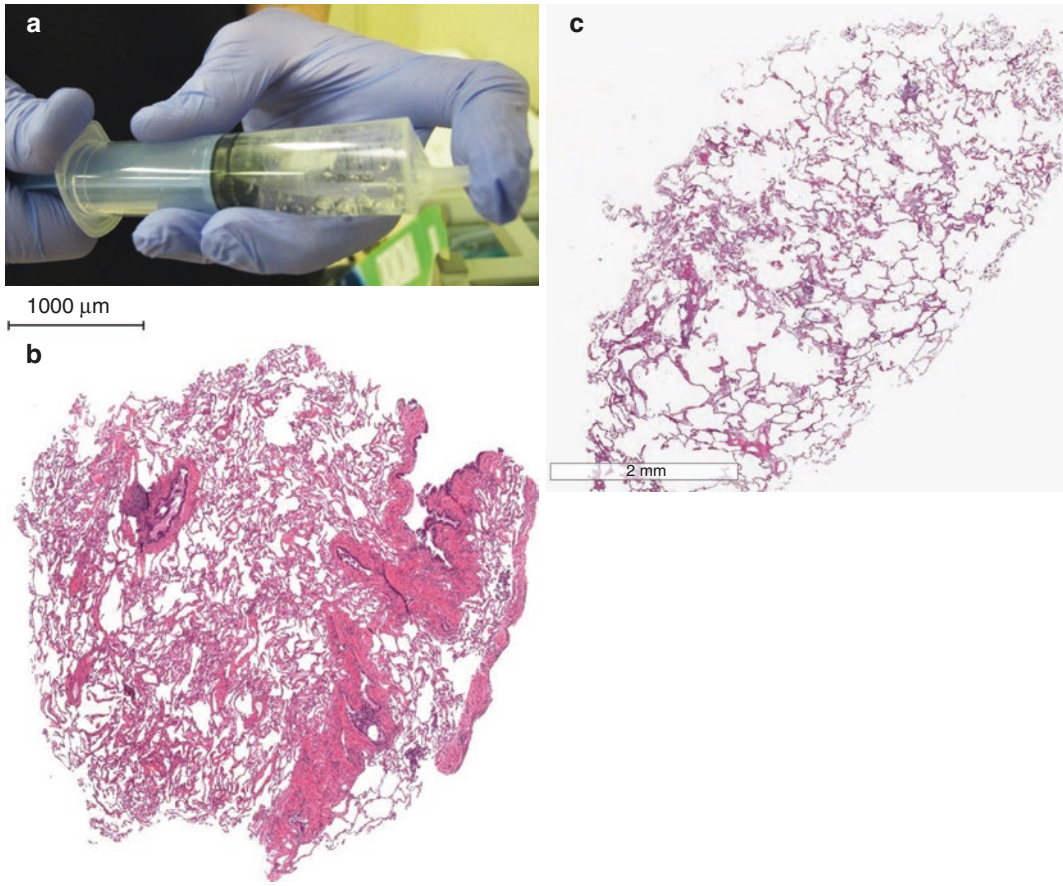

Fig. 7.1 Expansion of the thawed lung specimens. (**a**) Expansion of a thawed specimen in a 20-mL syringe by negative pressure before fixation with buffered formalin. (**b**) Poorly aerated alveoli in an uninflated specimen (HE, ×1). (**c**) Inflated alveoli obtained by application of negative pressure before fixation (HE, ×1)

pulmonary arteries and veins. Figure 7.3 reveals a more detailed three-dimensional scheme of a pulmonary lobule [9]. A pulmonary lobule measures 8–10 mm in diameter and is encircled by interlobular veins. One lobule contains about 3–5 acini, and a terminal bronchiole is located at the entrance to the acinus; respiratory bronchioles are located in the subacinar level. Red circle area may be sampled by TBLC.

The area encircled in green in the paraffin-embedded tissue is sampled by TBLC; it contains the terminal bronchiole, respiratory bronchioles, interlobular (interacinar) septa, and alveoli (Fig. 7.4). Pathological diagnosis is based on a clear understanding of the normal lung architecture, especially in view of the patchy distribution of some diseases, e.g., usual interstitial pneumonia (UIP)/idiopathic pulmonary fibrosis (IPF).

7.1.3 Pathological Diagnosis of UIP Based on the Pulmonary Architecture

7.1.3.1 UIP Diagnosed in SLB Specimens

Pathology of UIP is characterized by dense fibrosis with architectural distortion, predominant subpleural and/or paraseptal distribution of fibrosis, patchy involvement of the lung parenchyma by fibrosis, fibroblastic foci, and absence of features to suggest an alternate diagnosis [7, 10].

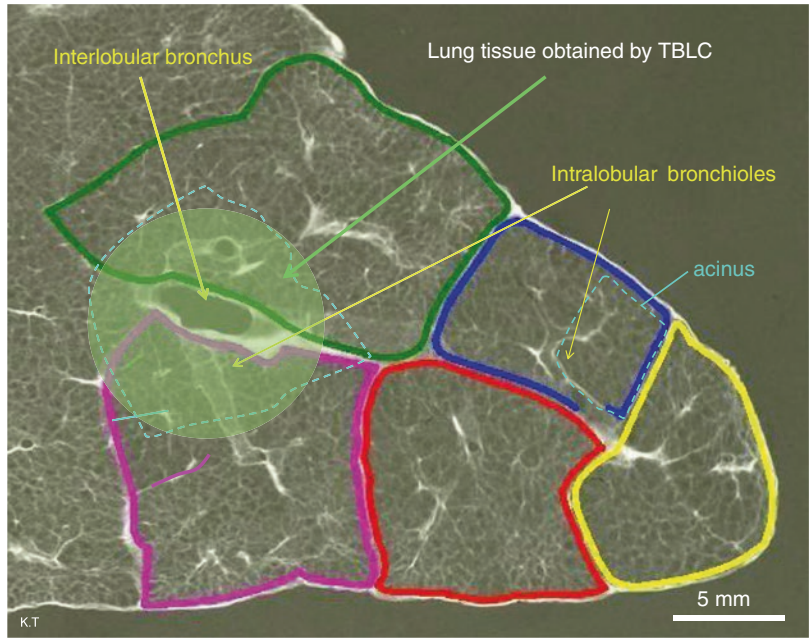

Fig. 7.2 Peripheral lung tissue. Softex image of normal peripheral lung tissue containing several lobules. The area encircled in green reveals the area possibly sampled by cryobiopsy and includes a membranous bronchiole, interlobular septa, veins, and arteries (Courtesy of Dr. H. Itoh, Fukui University)

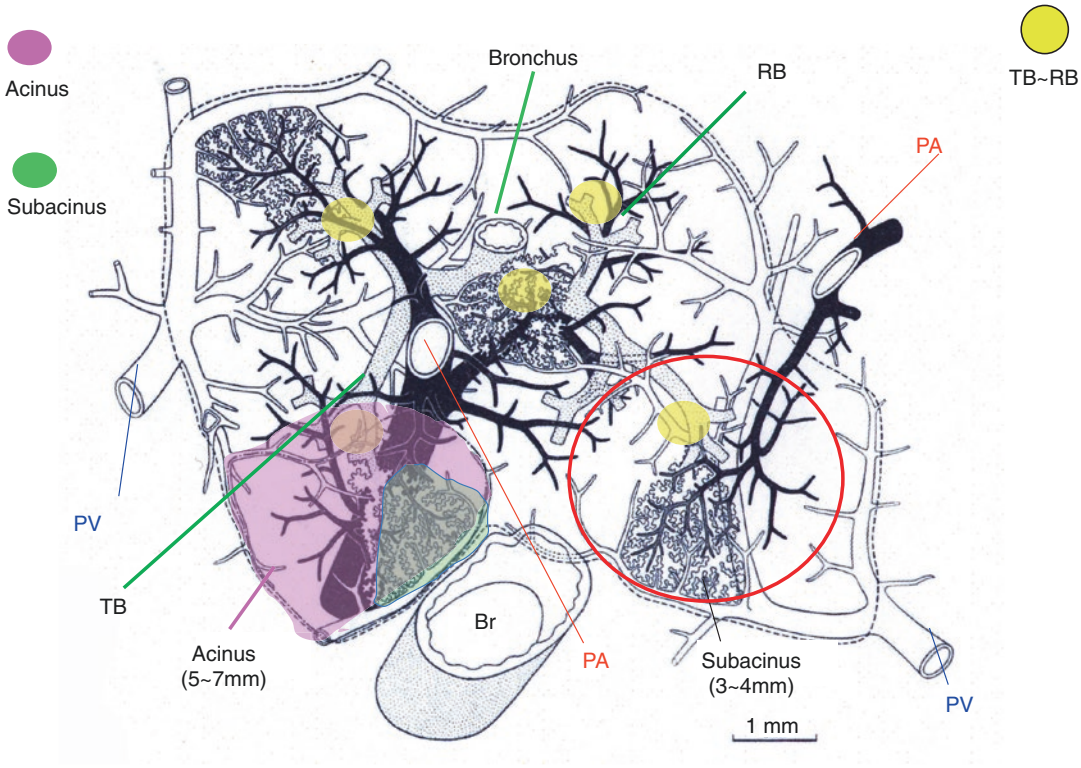

Fig. 7.3 Scheme of a pulmonary lobule. Scheme of a pulmonary lobule measuring 8–10 mm in diameter encircled by interlobular veins. Each lobule contains 3–5 acini (Permission from Iwanami Publisher, Tokyo, Japan). Area encircled in red may be sampled by cryobiopsy. *TB* terminal bronchiole, *RB* respiratory bronchiole

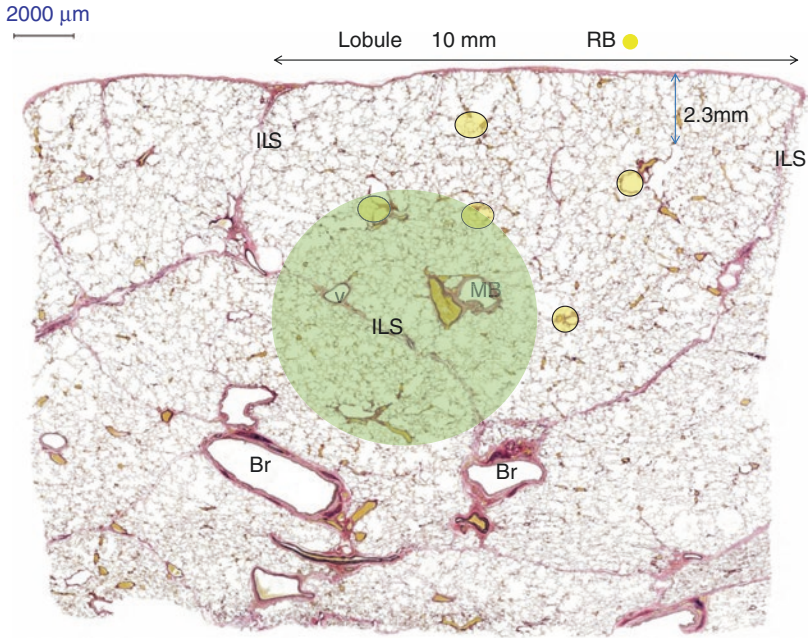

Fig. 7.4 Paraffin-embedded normal pulmonary lobule. Area encircled in green indicates the area sampled by cryobiopsy (EVG, ×1)

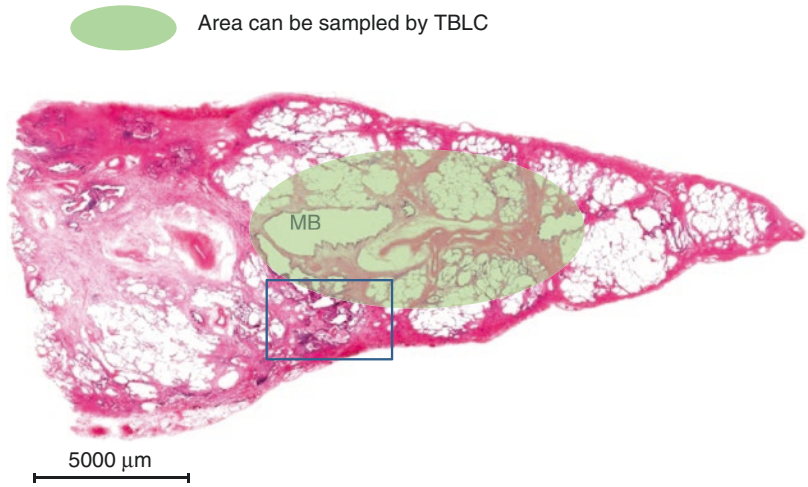

Fig. 7.5 Surgical lung biopsy specimen of UIP/IPF. Surgical lung biopsy specimen from the lower lobe with UIP/IPF, showing subpleural and paraseptal fibrosis alternating with normal alveoli. A square area shows microscopic honeycombing (HE, ×1)

Figure 7.5 reveals subpleural and paraseptal fibrosis with normal alveoli, consistent with the typical UIP pattern, in an SLB specimen. If TBLC were performed, structures in the area encircled in green can be obtained. The encircled area in Fig. 7.6, if obtained by TBLC, shows paraseptal fibrosis and peribronchiolar fibrosis with fibroblastic foci and alternating normal alveoli, consistent with UIP, even without pleural or subpleural fibrosis.

In TBLC specimens, honeycomb lesions cannot be easily observed, as seen in SLB specimens. The square area in Fig. 7.5 reveals microscopic honeycombing. Figure 7.7 reveals the structures shown in the square of Fig. 7.5 in greater detail; the area stained by EVG shows perilobular alveolar collapse, bronchiolar epithelialization of dilated alveoli, and traction bronchiolectasis. The area encircled may be sampled by TBLC is corresponding to microscopic honeycombing.

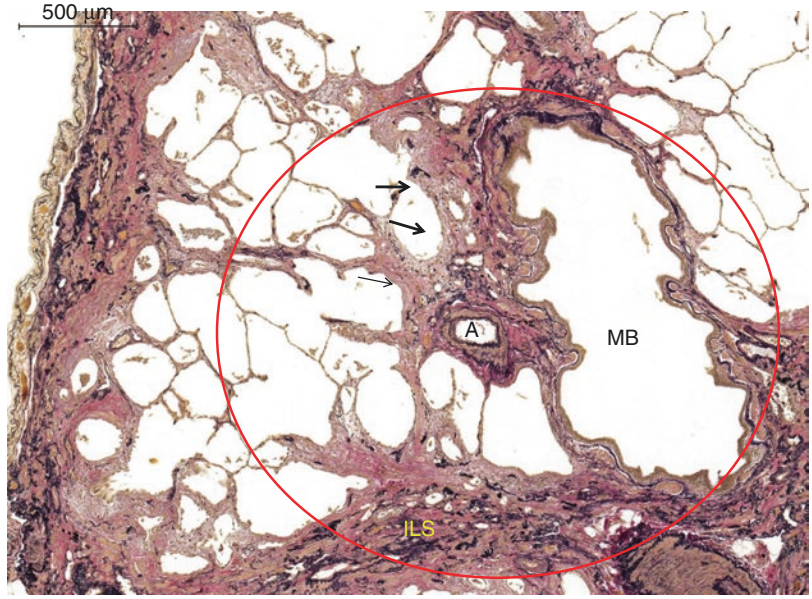

Fig. 7.6 A part of lobule of UIP. Paraseptal and peribronchiolar fibrosis with fibroblastic foci (arrows) are the hallmarks of UIP. This area is a part of Fig. 7.5 (EVG ×2.5). The circled area may be sampled by cryobiopsy, even in the absence of pleural and subpleural fibrosis

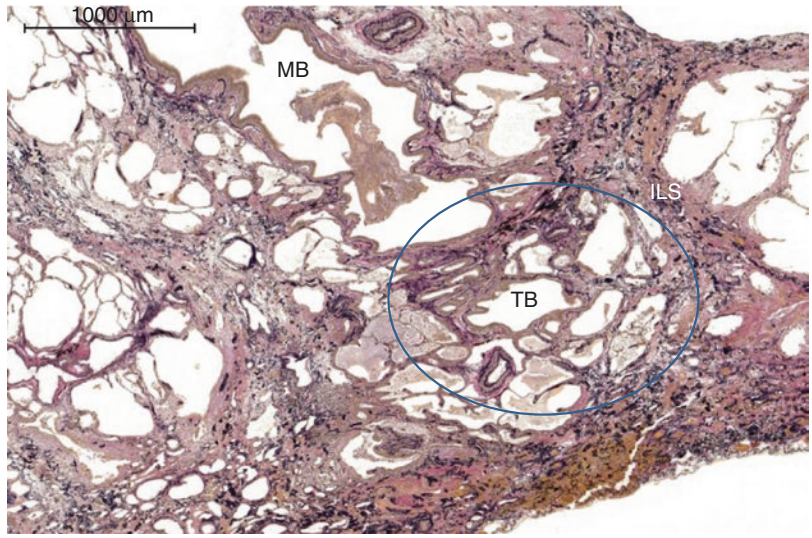

Fig. 7.7 Microscopic honeycombing. Microscopic honeycombing shows perilobular collapsed alveoli, bronchiolar epithelization, and traction bronchiolectasis. The encircled area, i.e., a part of microscopic honeycombing, may be sampled by cryobiopsy (EVG, ×2.5). *MB* membranous bronchiole, *TB* terminal bronchiole, *ILS* interlobular septum

7.1.3.2 UIP Diagnosed in TBLC Specimens

Figure 7.8a shows dense patchy fibrosis alternating with normal alveoli, containing two subacini, which are more clearly demonstrated by EVG staining, because of interlobular septum in the center (Fig. 7.8b) and fibroblastic foci (Fig. 7.8b, c).

Thus, pathological diagnosis of UIP by TBLC can be made with some degree of confidence [3, 5]. However, the histologic features in a small area of the lung cannot represent the entire pathological events. Thus, care must be ensured to avoid overdiagnosis. Patchy fibrosis in the pulmonary lobule can be observed in many clinical settings. Fibrosis apposed to the bronchovascular sheath or in the periacinar region is diagnostic of UIP. Microscopic honeycombing can be detected by TBLC. However, peribronchiolar

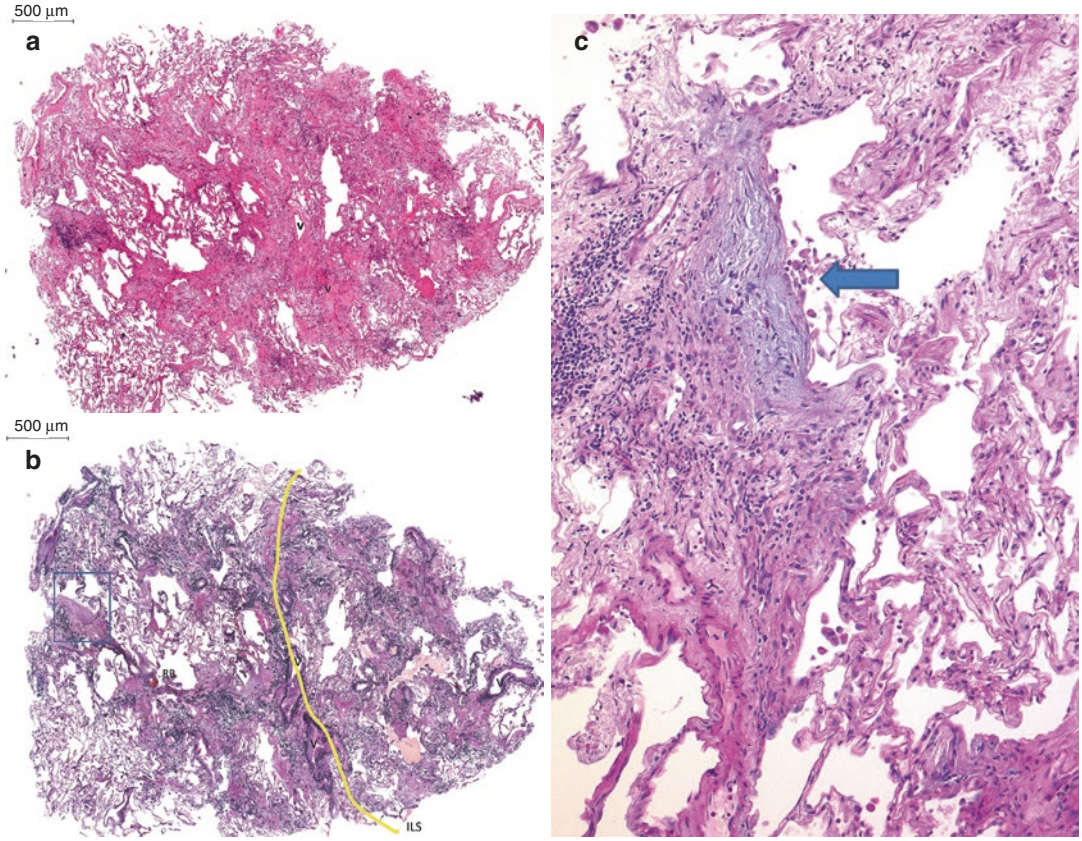

Fig. 7.8 UIP in cryobiopsy. (**a**) Cryobiopsy from the lower bronchus shows dense patchy fibrosis alternating normal alveoli (HE, ×4). *V* interlobular vein. (**b**) Fibrosis is mainly apposed to the interlobular septum and perivenular area (EVG, ×4). (**c**) Fibroblastic focus (*arrow*) is located on the old fibrosis (square of **b**), clearly demonstrated by Alcian blue staining (PAS-Alcian blue, ×10)

metaplasia, which is usually observed around bronchioles, must be differentiated from microscopic honeycombing.

7.2 Conclusion

TBLC can be safely performed for the diagnosis of diffuse interstitial lung disease (ILD) and provides reliable pathological diagnosis, potentially enabling prompt decision on the appropriate therapy.

However, there are still limitations of TBLC, as compared to SLB, for the pathological diagnosis of ILD, because of the limitation of the area from which samples can be obtained (more central area) and a high frequency of discordance with the radiological diagnosis. Further studies of correlations between diagnoses by TBLC and SLB are needed to determine the degree of diagnostic confidence that can be obtained with TBLC.

References

1. Poletti V, Hetzel J. Transbronchial cryobiopsy in diffuse parenchymal lung disease: need for procedural standardization. Respiration. 2015;90:275–8.
2. Hetzel J, Maldonado F, Ravaglia C, Wells AU, Colby TV, Tomassetti S, Ryu JH, Fruchter O, Piciucchi S, Dubini A, Cavazza A, Chilosi M, Sverzellati N, Valeyre D, Leduc D, Walsh SLF, Gasparini S, Hetzel M, Hagmeyer L, Haentschel M, Eberhardt R,

Darwiche K, Yarmus LB, Torrego A, Krishna G, Shah PL, Annema JT, Herth FJF, Poletti V. Transbronchial cryobiopsies for the diagnosis of diffuse parenchymal lung diseases: expert statement from the cryobiopsy working group on safety and utility and a call for standardization of the procedure. Respiration. 2018;95:188–200.

3. Ravaglia C, Wells AU, Tomassetti S, Dubini A, Cavazza A, Piciucchi S, Sverzellati N, Gurioli C, Gurioli C, Costabel U, Tantalocco P, Ryu JH, Chilosi M, Poletti V. Transbronchial lung cryobiopsy in diffuse parenchymal lung disease: comparison between biopsy from 1 segment and biopsy from 2 segments-diagnostic yield and complications. Respiration. 2017;93:285–92.
4. Colby TV, Tomassetti S, Cavazza A, Dubini A, Poletti V. Transbronchial cryobiopsy in diffuse lung disease. Update for the pathologist. Arch Pathol Lab Med. 2017;141:891–900.
5. Tomassetti S, Wells AU, Costabel U, Cavazza A, Colby TV, Rossi G, Sverzellati N, Carloni A, Carretta E, Buccioli M, Tantalocco P, Ravaglia C, Gurioli C, Dubini A, Piciucchi S, Ryu JH, Poletti V. Bronchoscopic lung cryobiopsy increases diagnostic confidence in the multidisciplinary diagnosis of idiopathic pulmonary fibrosis. Am J Respir Crit Care Med. 2016;193:745–52.
6. Lynch DA, Sverzellati N, Travis WD, Brown KK, Colby TV, Galvin JR, Goldin JG, Hansell DM, Inoue Y, Johkoh T, Nicholson AG, Knight SL, Raoof S, RIcheldi L, Ryerson CJ, Ryu JH, Wells AU. Diagnostic criteria for idiopathic pulmonary fibrosis: a Fleischner Society White Paper. Lancet Respir Med. 2018;6:138–53.
7. Raghu G, Remy-Jardin M, Myers JL, Richeldi R, Ryerson CJ, Ledere DJ, Behr J, Cottin V, Danoff SK, Morell F, Flaherty KR, Wells A, Martinez FJ, Azuma A, Bice TJ, Bouros D, Brown KK, Collard HR, Duggal A, Galvin L, Inoue Y, Jenkins RG, Johkoh T, Kazerooni EA, Kitaichi M, Knight SL, Mansour G, Nicholson AG, Pipavath SNJ, Buendia-Roldan I, Selman M, Travis WD, Walsh S, Wilson KC, On behalf of the American Thoracic Society, European Respiratory Society, Japanese Respiratory Society, and Latin American Thoracic Society. Diagnosis of idiopathic pulmonary fibrosis. An official ATS/ERS/JRS/ALAT clinical practice guideline. Am J Respir Crit Care Med. 2018;198(5):e44–68.
8. Pajares V, Puzo C, Castillo D, Lerma E, Montero MA, Ramos-Barbon D, Amor-Carro O, Gil de Bernabe A, Franquet T, Plaza V, Hetzel J, Sanchis J, Torrego A. Diagnostic yield of transbronchial cryobiopsy in interstitial lung disease: a randomized trial. Respirology. 2014;19:900–6.
9. Matsumoto T. Lung. Chapter 10 in tissue and organ. In: Modern biology course 10. Tokyo: Iwanami Publisher; 1977. p. 315–72.
10. Raghu G, Collard HR, Egan JJ, et al. An official ATS/ERS/JRS/ALAT statement: idiopathic pulmonary fibrosis: evidence-based guidelines for diagnosis and management. Am J Respir Crit Care Med. 2011;183:788–214.